

Amphotericin B interactions with a DOPC monolayer. Electrochemical investigations

R. Stoodley^a, J. Shepherd^a, K.M. Wasan^b, D. Bizzotto^{a,*}

^aDepartment of Chemistry, University of British Columbia, Vancouver, BC, Canada V6T 1Z1

^bFaculty of Pharmaceutical Sciences, University of British Columbia, Vancouver, BC, Canada V6T 1Z3

Received 27 November 2001; received in revised form 16 April 2002; accepted 9 May 2002

Abstract

A model lipid membrane consisting of a monolayer of dioleoyl phosphatidylcholine (DOPC) adsorbed onto a Hg electrode has been used to study the interaction between the lipid and different formulations of Amphotericin B (AmB) [Fungizone® (FZ), Heated Fungizone (HFZ), and Abelcet®]. The lipid organizational order was measured by electrochemical methods [capacitance and metal ion (Tl⁺) reduction], characterizing the change in lipid order due to interaction with the drug. The mean size and number density of pores formed in the monolayer were estimated by fitting the reduction current transients to a random array of microelectrode model. This method was shown sensitive for investigation of the interaction of drugs with the DOPC monolayer. Abelcet was found to have a smaller disruptive effect on lipid order than FZ and HFZ. The formulations used to solubilize the AmB were also studied. Sodium deoxycholate used as a solubilizer in FZ displayed significant influence on lipid order similar to that observed for Abelcet. The lipid complex, used in Abelcet, did not significantly perturb the DOPC monolayer order. The lipid complex used in Abelcet may have an annealing or healing effect that buffers the disruption possible due to AmB. © 2002 Elsevier Science B.V. All rights reserved.

Keywords: Amphotericin B; Lipid; Dioleoyl phosphatidylcholine monolayer

1. Introduction

Amphotericin B (AmB) is a polyene macrolide antibiotic used to combat fungal infections in patients with impaired immune systems. Studies in this area are important because of the increased occurrence of fungal infections [1,2]. This increase is due in part to improved recognition and diagnosis of fungal infections, but also to the prolonged survival of patients with defects in their host defense mechanisms, including patients with cancer, organ transplant recipients, diabetics, and patients with AIDS [3,4]. In these patients, invasive fungal infections may account for as many as 30% of deaths [4,5].

The treatment of systemic fungal infections has relied upon drugs that tend to have significant in vivo toxicity. AmB's use is limited due to its systemic side effects [6,7] (fever and chills) and renal toxicity (which limits the duration of therapy). The observed toxicity results from a similarity of drug interaction with mammalian and fungal

cells, and its effectiveness as therapy relies upon the selectivity of the destructive interaction toward fungal cells. The mechanism of action of polyene antibiotics and the role played by the components of the cell membrane (lipid, sterol, membrane protein) is still under discussion, but generally, interaction between the sterol and the antibiotic is considered important [6,8]. The major sterol component is cholesterol for the mammalian cell and ergosterol for the fungal cell. Differences in the interaction between the AmB and each sterol have been proposed [6,7] to be the origin of the effectiveness of the treatment although this sterol hypothesis is still under study.

It is believed that AmB initially adsorbs onto the cell membrane and forms non-conductive pre-pore complexes [9,10]. AmB then interacts with the sterol in the cell membrane creating ion channels and pores resulting in cell lysis and death. This process has been recently studied using AFM [11]. Studies show that the efficacy of AmB is based on its strong interaction with ergosterol in fungal membranes as compared to the weaker interaction with cholesterol in mammalian membranes, resulting in a differentiated response [9].

* Corresponding author. Tel.: +1-604-822-6816; fax: +1-604-822-2847.
E-mail address: bizzotto@chem.ubc.ca (D. Bizzotto).

AmB is amphipathic having low solubility in water. It exists in many forms (monomers and aggregated structures) in aqueous media for concentrations above 1 μM , the critical aggregate concentration [9]. Due to its amphipathic nature, AmB requires solubilization for administration. Fungizone (FZ) (Bristol-Myers Squibb, New Jersey) is the most widely used formulation in which AmB is complexed with a detergent (deoxycholate). It has been suggested that the aggregated forms of the drug are toxic to both ergosterol- and cholesterol-containing membranes, while the monomer specifically porates ergosterol-containing membranes. The absorption spectra of monomer and self-associated forms of AmB are different and a blue-shifted band has been observed for aggregated molecules [12]. Heating the AmB/deoxycholate complex (20 min at 70 °C) creates a super-aggregated form of AmB, Heat-Treated Fungizone (HFZ), which appears to have a reduced toxicity [13,14]. One hypothesis explaining the HFZ results suggests that the super-aggregated form of AmB does not form channels in the membrane, unlike the aggregated form, but exists near the membrane, releasing monomers of AmB which selectively damage fungi membranes, thereby maintaining the drugs efficacy. AmB complexed with lipids (Abelcet) or contained within liposomes have decreased toxicity [15–19]. These formulations have similar efficacy to FZ but remain expensive and inaccessible to most patients.

Although AmB has been used clinically for many years, basic physical–chemical data on its aggregation state in solution and the method of incorporation into the cell membrane are not clear. For example, the sterol hypothesis claims that the presence of sterol is critical to the formation of the pore. Some studies have shown that pores are created even in sterol-free membranes [20,21] and recently, pores have been found in sterol-free membranes that were under osmotic stress [22]. These conflicting observations and hypotheses demonstrate the need for tools and simple experimental models for measurement of the drug/lipid/sterol interaction under varying conditions.

A number of different avenues have been taken toward understanding the molecular interactions that play a role in the mechanism of AmB action on fungal and mammalian cell membranes. These generally fall into two categories: floating monolayer (Langmuir trough) studies and studies on lipid bilayers (vesicles or BLM). In both cases, basic physical–chemical data regarding the interactions of the drug with the lipid and sterol components of the membrane have been obtained. Characterization of interactions between AmB, lipid and sterol was performed in a Langmuir trough [23–31]. These fundamental studies were useful for defining the nature of AmB interaction with lipid and sterol, although a floating monolayer is not a mimic of a biological membrane.

The influence of AmB on lipid bilayers, either as BLM or liposomes, sterol-free or containing either cholesterol or ergosterol was also extensively studied [20,22,32–39]. Formation of ion-specific and nonspecific pores in the lipid

bilayer was observed through measurement of ionic or molecular flux. The type and concentration of sterol in the membrane was also manipulated. These studies confirmed the formation of pores in the lipid bilayers due to sterol/AmB complex. Pores were also observed in sterol-free liposomes that were subjected to osmotic stress, indicating a need for more fundamental studies.

The interaction of the anti-fungal drugs with membranes *in vivo* is a complicated problem and model membranes facilitate the investigation of these interactions. We shall describe an electrochemical technique for studying the lipid/AmB interaction performed on dioleoyl phosphatidylcholine (DOPC) monolayer. A DOPC monolayer floating on an aqueous solution is deposited onto a Hg drop electrode. The DOPC monolayer models the outer leaflet of a biological membrane since the alkyl tails are adsorbed onto the metal surface and the head groups are in contact with the aqueous phase [40,41]. Deposition onto a conductive surface allows the use of electrochemical techniques for characterization and control of the adsorbed monolayer. The electrochemical properties of phospholipid monolayers of DOPC adsorbed onto mercury surfaces have been investigated using capacitance measurements [40–45]. An increase in the minimum capacitance will indicate an increase in the defect content of the adsorbed lipid layer, which can be correlated to interaction with compounds in the aqueous phase. In addition, these layers display multiple states that interconvert, at specific potentials, through phase transitions that are manifested as peaks in the capacitance measurements. These peaks are sensitive to changes in the organization of the adsorbed layer, to the composition of the layer and to interaction with surface active agents in solution, such as therapeutic drugs like AmB. The height and width of these peaks contain information about the kinetics of the adsorption/desorption or reorientation (condensation) process [46–48] and therefore can be used as an indirect measurement of the organizational properties of the adsorbed lipid layer. These tools are particularly useful since slight defects in the lipid layer will be reported by the electrochemical measurements, allowing us to investigate the pre-pore formation events.

The integrity of the adsorbed DOPC layer and the phase transition regions was further characterized utilizing metal ion (Ti^+) reduction. These metal ions are reduced at the Hg surface to form an amalgam, but first they must penetrate through the lipid layer. This affords us the ability to measure the permeability of the lipid layer. In addition, the potential drop across the adsorbed layer controls this permeability [42]. The lipid layer phase transition is preceded by the creation of various defect regions that allow the metal ion facile access to the Hg surface. The creation of these defects is due to stress caused by the imposed potential drop across the monolayer, not unlike the effects of osmotic stress. In both cases, pores are created in the lipid layer, due to osmotic or interfacial tensions. The rate of the metal ion penetration through the layer (measured as current) is correlated to the

size and density of pores in the lipid layer. The creation of these pores is a function of the lipid layer's organizational properties that are modified by interaction with the drug.

We describe the use of a model membrane system to study three different formulations of AmB and their interaction with the lipid monolayer. The electrochemical response of the lipid/Hg model was utilized to characterize the changes in the monolayer organization due to interaction with AmB formulations. The model system is a monolayer of DOPC, and as such, is not an ideal model of a cell membrane. The advantage using this model is in its characterization of lipid organization and of the subtle changes that may exist due to peripheral interaction with the drug in solution. In addition, the size and density of pores created through a combination of interaction with the drug and the potential drop across the DOPC layer can be extracted. The questions that can be addressed with this methodology include: how do FZ, HFZ and Abelcet modify sterol-free monolayers; how can this interaction be quantified and what new insights can be gained on the possible mechanism of action (mechanism of this disruption).

2. Materials and methods

2.1. Formulation preparation

FZ was prepared according to manufacturer's directions: FZ was supplied as a lyophilized powder consisting of 50 mg AmB, 41 mg sodium deoxycholate, and 20.2 mg sodium phosphates made up to 10 ml volume with MilliQ water. This stock solution was diluted 5:1 with MilliQ water before use. HFZ was prepared by heating the diluted FZ solution to 70 °C for 20 min. Sodium deoxycholate (Sigma ultra grade) solution (0.85 mg/ml) was prepared in MilliQ water. Abelcet® (The Liposome Company, New Jersey) was supplied as 20 ml volume containing 100 mg AmB, 68 mg L- α -dimyristoylphosphatidylcholine (DMPC), 30 mg L- α -dimyristoylphosphatidylglycerol (DMPG), and 180 mg sodium chloride used as received. An Abelcet blank was prepared to have the same composition as Abelcet, but without the AmB. DMPC and DMPG were from Avanti Polar Lipids (Alabaster, AL) and KCl (Fluka) was used instead of NaCl. AmB is used as a generic term to describe any of FZ, HFZ, and Abelcet. AmB was introduced into the cell by injecting by syringe an aliquot into the electrolyte (70 ml of 0.1 M KCl) and stirring gently for 30 s with a magnetic stir bar. FZ and Abelcet concentrations were expressed as percentages of the normal adult therapeutic dose (TD) specified by the manufacturer (0.5 and 5 mg l⁻¹, respectively) in an attempt to mimic physiological conditions. The actual concentrations of AmB in the subphase at the TD were 0.54 and 5.4 μ M, respectively. Sodium deoxycholate was introduced in concentrations equivalent to the deoxycholate concentration in each percentage therapeutic dose of FZ. The same procedure was used for lipid mixture that comprises the Abelcet blank.

2.2. Electrochemical apparatus and methods

A monolayer of DOPC (semi-synthetic grade, Lipid Products UK) was formed on the surface of 0.1 M KCl (Fluka, calcined 500 °C, prepared in 18.2 M Ω MilliQ water and deaerated with argon) as described previously [49,50]. Briefly, 8 μ l of 2 mg/ml DOPC dissolved in pentane is introduced onto the surface of deaerated electrolyte. The pentane evaporates leaving a monolayer of DOPC in equilibrium with bulk phase DOPC present as droplets. The DOPC monolayer exists at its equilibrium spreading pressure ($\Pi^e=50$ mN m⁻¹) which is the greatest surface concentration that can be achieved while remaining in a thermodynamically stable phase [51]. This procedure ensures a consistent DOPC surface concentration, even if material is lost to the walls of the glass cell. The floating lipid monolayer is deposited onto a Hg drop (Fig. 1) under potential control by passing the drop through the DOPC/electrolyte surface. A hanging drop mercury electrode (WK2, Polish Academy of Sciences), filled with triple distilled mercury (DFG Mercury) was used. The capillaries were silanized using 4% dimethyl-dichlorosilane in trichloroethane before filling with Hg. The Hg-filled capillary was cleaned before use by dipping into a sulfuric/nitric acid mixture. This DOPC/Hg interface was configured as the working electrode in a three-electrode arrangement. The SCE reference electrode was connected to the working solution through a salt bridge. The counter electrode was a platinum coil cleaned by flame annealing.

The electrochemical measurements were made with a potentiostat (FHI) used with a lock-in amplifier (PAR 5210) and data were recorded with a National Instruments (12 bit, 1.25 MHz) data acquisition system and Labview. In this paper, all potentials are quoted versus the saturated calomel electrode (SCE). For capacity experiments, the cell was stimulated with an AC waveform (70 Hz) superimposed on a voltage ramp (scan rate 5 mV/s). The amplitude of the AC perturbation was 2 mV rms, smaller than in previous studies [42] chosen for its decreased non-linear response in the region of the pseudo-capacitance peaks. The capacity was

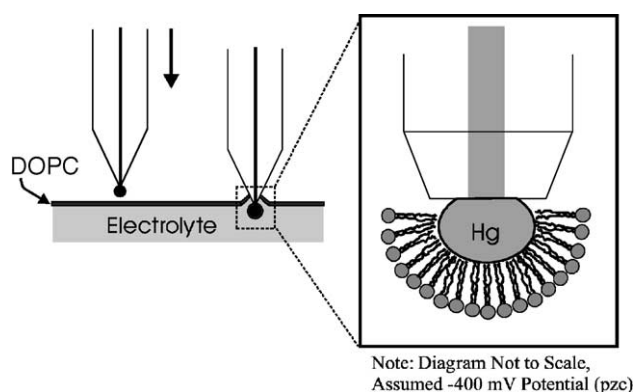


Fig. 1. Schematic representation of the experimental setup illustrating the Hg drop electrode and the method of depositing a lipid monolayer.

calculated from the out-of-phase and in-phase components of the current assuming a series RC circuit.

Chronoamperometry was used to characterize Tl(I) reduction in the potential region leading to and covering the first phase transition. The Tl(I)/Tl(Hg) couple is kinetically fast on the bare mercury electrode surface [52] and inhibition of Tl⁺ reduction results from blocking of the electrode surface by the adsorbed DOPC monolayer. Therefore, changes in the characteristics of the faradaic reaction can be used as a measure of the permeability of the DOPC monolayer. The potential (E) was held at -0.25 V for 3 s and then stepped to successively more negative values (up to -1.2 V) for 1 s for both the DOPC covered and uncovered electrode surface. Finally, the potential was stepped to -0.2 V for 10 s to allow any Tl(Hg) to become oxidized and diffuse out of the Hg. The current was recorded at a 20-kHz sampling frequency with a 10-kHz low-pass filter.

3. Results and discussion

3.1. Capacitance measurements

Characterization of the adsorbed layer relies upon capacitance measurements which is a sensitive but averaging technique. DOPC monolayer adsorbed onto Hg displays a minimum capacitance of $1.85 \mu\text{F cm}^{-2}$ at potentials of the uncharged Hg surface, and any increase from this value indicates a decrease in monolayer order or the introduction of defects. Potential-induced phase changes are also observed and are a sensitive measure of monolayer order. These phase changes are manifested as pseudo-capacitance peaks (-0.965 and -1.025 V/SCE). Previous work [42] has shown that the phase change was preceded by potential-induced defect formation, from which the new phase starts to grow. The potential range through which the phase change occurs will depend upon the energetics of the growth of the new phase from the potential-induced defects. If all defects are energetically homogeneous, which would be expected for a well-ordered phase, the phase change will occur at a single value of the potential. If the monolayer is disordered, the potential-induced defects will be energetically heterogeneous and the phase change will occur over a range of potentials, causing the pseudo-capacitance peaks to be broad and less intense. The height of the peaks is therefore a sensitive indication of the lipid monolayer organization. The lipid monolayer organization was interrogated through the measurement of the pseudo-capacitance peaks (phase change kinetics) and minimum capacitance of the monolayer. These two criteria allow us to indirectly probe interaction of DOPC with the AmB formulations, and the corresponding control solutions. We expect that interaction with the DOPC head groups may not change the minimum capacitance significantly, but would result in modification of the capacitance peaks. On the other hand,

direct insertion into the DOPC monolayer would increase the minimum capacitance of the layer, as well as decrease the height of the phase transition peaks.

The differential capacitance–potential measurements are shown in Fig. 2 for DOPC alone, and with additions of 80% of therapeutic dose of deoxycholate, FZ, HFZ, Abelcet, and Abelcet blank. The DOPC layer was deposited onto the Hg electrode at -0.4 V/SCE and the potential is scanned negatively up to -1.2 V/SCE, just beyond the capacitance peaks which signal the phase changes. These curves are shown in solid line and represent the *as-deposited* layer characteristics. In other words, the DOPC layer deposited onto the Hg drop is representative of the layer on the gas/solution interface after exposure to the subphase with additions of drug. The floating DOPC monolayer (at Π^e) is well organized (i.e. not significantly perturbed) and interaction with AmB models the interaction with a cell membrane that is free of defects or pores. Scanning the potential negatively introduces a stress (potential) to the system which is used to interrogate the integrity of the deposited monolayer. The layer becomes porated and strongly defective at these negative potentials containing many holes/defects with which AmB can interact. The potential is then scanned positively, back to the initial value of potential and the characteristics of the *reformed* layer measured (represented by the dashed line in Fig. 2). This scan is representative of the reformation of a possibly defect-free lipid layer from a lipid layer that was stressed and defective. Reforming the defect-free monolayer will be hampered by incorporation or interaction with the drug, which will be apparent in the height of the capacitive peaks and via the minimum capacitance measurements.

The DOPC layer (Fig. 2c) has a stable minimum capacitance of $1.85 \mu\text{F cm}^{-2}$ and a peak height of $100 \mu\text{F cm}^{-2}$ for the most positive and intense peak. These two characteristics are the same regardless of the potential scan direction, illustrating the ideal character of this monolayer making it a suitable choice for investigations of drug/lipid interaction. These characteristics were always achieved before addition of any drug to the subphase, and therefore represent a convenient control ensuring the same starting DOPC monolayer. The addition of 80% of the TD of Abelcet (Fig. 2e) into the subphase elicits a drop in the peak height for both the *as-deposited* and *reformed* layers. The *as-deposited* layer minimum capacitance was not strongly perturbed but a slight increase in the monolayer capacitance was measured for the *reformed* layer. Abelcet is composed of a lipid complex of AmB/DMPC/DMPG, and the appropriate control of DMPC/DMPG was also examined (Fig. 2f). The Abelcet blank measurements were identical with the baseline DOPC results, indicating that the lipid complex in solution had little influence on the lipid monolayer. The changes observed for Abelcet are due to the presence of AmB which enhances the interaction with the lipid monolayer. The lipid complexed AmB, and the lipid blank seem to interact only with the DOPC head groups, thereby

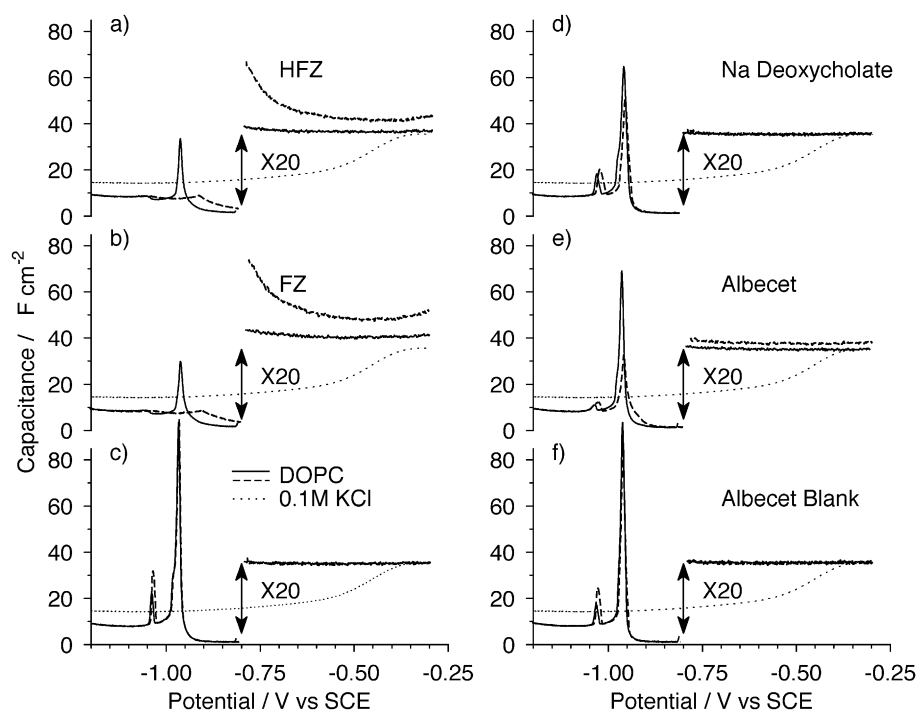


Fig. 2. Capacitance measured for Hg/0.1 M KCl (.....) and DOPC-coated Hg drop in contact with 80% TD of various AmB formulations (as deposited —, reformed - - - - -): (a) HFZ, (b) FZ, (c) only DOPC, (d) deoxycholate (blank solution for FZ group), (e) Abelcet, (f) Abelcet blank composed of DMPG/DMPC. The capacitance was calculated assuming a series RC circuit, measured using 5 mV/s, 70 Hz, 2 mV rms.

influencing the phase change but not introducing defects in the DOPC layer at -0.4 V/SCE. Abelcet has been shown to have low *in vivo* toxicity though remaining effective at the recommended TD. These results certainly illustrate the limited influence of this formulation on the disruption of the pure DOPC monolayer, in contrast to the FZ results presented below.

Fig. 2b illustrates the strong influence FZ had on the DOPC monolayer. The capacitance of the as-formed layer is $1.9 \mu\text{F cm}^{-2}$ which is larger than the DOPC control. The disruption of the DOPC monolayer maybe due to a strong interaction of non-conductive pre-pore complexes of AmB with the membrane [9,10]. The phase change peaks are significantly altered, decreased to $30 \mu\text{F cm}^{-2}$ for the as-deposited layer and were not measurable for the reformed layer. The minimum capacitance of the reformed layer is much larger and no longer independent of potential, having a minimum around -0.4 V/SCE with a value of $2.2 \mu\text{F cm}^{-2}$. The alteration to the layer is significant. A similar interaction of HFZ with the lipid layer was also observed (Fig. 2a). FZ is a mixture of AmB and deoxycholate. Therefore, a deoxycholate control was also measured (Fig. 2d). The minimum capacitance of the as-deposited layer is the same as the DOPC control, although the peak was reduced to $60 \mu\text{F cm}^{-2}$. The reformed layer demonstrated a similar decrease in peak height, but the minimum capacitance remained at $1.85 \mu\text{F cm}^{-2}$. Deoxycholate is an anionic surface active agent that would tend to interact with the

DOPC head groups. It is evident from the capacitance measurements that deoxycholate only interacts with the lipid in a peripheral way, slightly influencing the potential-driven lipid phase change, but not increasing the minimum capacitance. The AmB/deoxycholate complex (FZ or HFZ) had a significant disrupting effect on the layer. Initially, AmB strongly interacts with the lipid monolayer. Once holes are created in the lipid layer through negative potential excursion, AmB inserts itself into the lipid matrix causing a significant decrease in lipid order and a large number of defects preventing the reformation of a defect-free DOPC monolayer.

Fig. 3 compiles capacitance peak data and minimum capacitance data as a function of the percentage of TD or equivalent for the five solutions used. The minimum capacitance for the as-deposited layer increases with sub-phase concentration for only the FZ and HFZ. The peak capacitance changes in a more complex manner. The largest changes observed are again for the FZ and HFZ with a sharp decrease from 100 to $35 \mu\text{F cm}^{-2}$. The FZ control (deoxycholate) also influences the peak capacitance, but in a less dramatic manner, decreasing to $60 \mu\text{F cm}^{-2}$. This again indicates that the largest changes to the DOPC monolayer were observed in the presence of AmB. In contrast to these large changes, the Abelcet blank only causes a decrease in the peak capacitance at the lower concentrations, but essentially no significant decrease was observed. The decrease in peak capacitance for Abelcet was larger than for the Abelcet

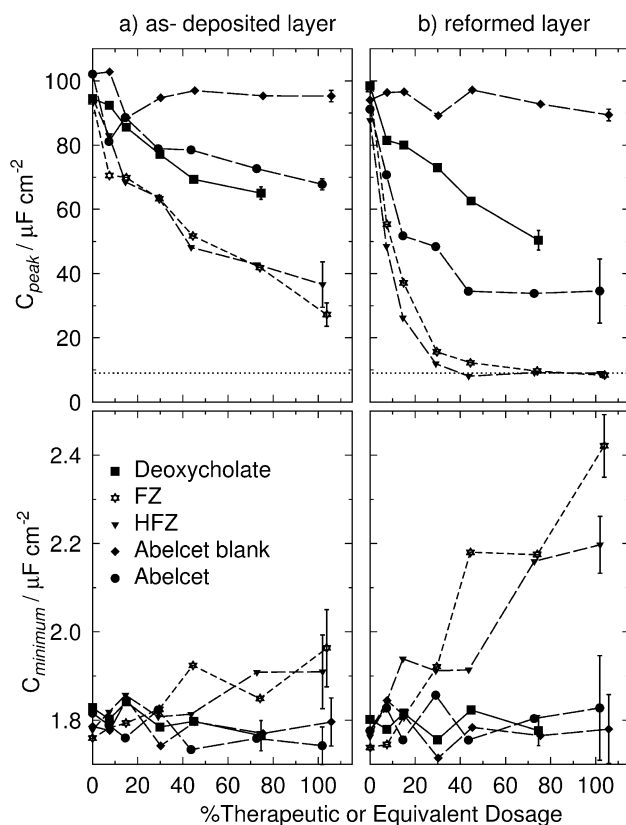


Fig. 3. Summary of capacitance data (minimum capacitance measured between -0.6 and -0.35 V/SCE, and maximum peak capacitance) for the various formulations of AmB: (a) the as-deposited DOPC layer, (b) the reformed DOPC layer as a function of the fraction of TD or equivalent. Representative errors for the capacitance measurements are shown. The dotted line in the top panels represents the baseline capacitance values.

blank, similar to that observed for deoxycholate. These results reveal that Abelcet induces smaller changes or disorganization in the as-deposited DOPC monolayer when compared to FZ or HFZ. These results for the as-deposited layers can be used to estimate the effect of the drug on sterol-free cell membranes which do not experience significant stress which would result in weak areas within the membrane (similar to the effect of osmotic stress).

The matrix in which the AmB exists also seems to have a significant influence. Comparing the Abelcet and FZ blanks clearly demonstrates this effect. Deoxycholate influences the DOPC layer in a manner that appears similar to Abelcet itself, while the Abelcet blank does not interact or disrupt the lipid monolayer. These observations suggest that the solubilizing agent may also cause significant damage to the membrane in addition to the effect of AmB.

Scanning the potential to the negative limit introduces pores or defects into the adsorbed lipid monolayer. Once porated, reformation of the adsorbed layer provides further information on the interaction of the drug with defective regions of the DOPC monolayer. The capacitance peaks measured for the reformed layer show that FZ and HFZ

significantly affect the readsorption of the layer. The capacitance peak disappears at concentrations above 40% of the TD. Deoxycholate also decreases the peak heights but less efficiently than FZ or HFZ. Abelcet also strongly interacts with the defective layer but the response is saturated at $35 \mu\text{F cm}^{-2}$, illustrating that the lipid complexed AmB has a limited influence on the defective monolayer. The Abelcet blank has no influence on the reformation of the DOPC monolayer. The excess lipid present in the Abelcet may act to mitigate the destructive influence of AmB, or the lipid may shield the sterol-free DOPC monolayer from interaction with the complexed AmB.

Support for the general discussion above was also observed with the minimum capacitance for the reformed layer. The only significant increases are observed for FZ and HFZ, while the other formulations did not modify the capacitance of the re-formed monolayer. This suggests that FZ and HFZ have components that are incorporated within the lipid monolayer, while Abelcet, Abelcet blank, and deoxycholate are displaced from the monolayer resulting in a DOPC layer similar to that first deposited. These indirect observations of the effect of AmB on a one-component lipid layer, in its various formulations, are somewhat correlated to the *in vivo* toxicity results [53]. In these cases, the FZ family has a strong toxic effect on renal cells which limits the amount of drug that can be administered. Complexation of AmB with lipid demonstrates a lower toxicity but maintains its efficacy though requiring a larger dose. The lowered toxicity may result from the buffering or healing effect of the excess lipid.

3.2. *Tl* reduction measurements

The capacitance measurements provide clues to origin of the toxicity of AmB by investigating the effect of the drug on the lipid organization in an indirect, though sensitive manner. AmB incorporates into the cell membrane creating holes through which the cell contents are lost, resulting in cell death. This process has been thought to occur for sterol-containing membranes, and for membranes lacking sterol if under osmotic stress [22]. A porated lipid monolayer can be characterized by measuring metal ion reduction through the monolayer yielding the mean size and number density of the holes assuming a random array of microelectrode model [54]. Diffusion to a microelectrode occurs in a hemispherical fashion, yielding currents that are larger than what would be expected for linear diffusion to an electrode of similar size. Diffusion to an array of microelectrodes would proceed through the initial hemispherical diffusion characteristic at short times. Once neighboring hemispheres overlap, the diffusion characteristic changes evolving toward linear diffusion. Therefore at long times, measurement of the reduction current would yield the same result for an uncovered electrode surface, as for one covered with pinholes. The current transient can be used to determine the average size and density of the pinholes under constraints of the model system.

This approach can estimate the hole radius in a restricted range, limited by experimental factors. The smallest measurable model pore sizes are typically $0.1\ \mu\text{m}$, due to overlap of the capacitive and faradaic currents at short times ($<5\ \text{ms}$). The upper limit is determined by the time at which the hemispherical diffusion layers sufficiently overlap resulting in linear diffusion. For situations where the density or size of the pinholes is large such that linear diffusion is achieved before the short time limit, no measurement of the pore size is possible since only linear diffusion is observed. The fraction of the surface covered with lipid can be determined by calculating the total area occupied by the holes. This is only an estimate of the true coverage since metal ions can penetrate regions of the monolayer that are thin especially with sufficient overpotential [55–58]. The average radii and density of pores are useful parameters that can be used to explore the changes in the monolayer after interaction with the drug, but the absolute size of the pores must be interpreted with caution. The current transient for diffusion to an array of microelectrodes cannot be easily distinguished from a current transient for a chemical step preceding an electron transfer. This CE reaction has been used in the study of transport through Gramicidin incorporated into a DOPC monolayer which was adsorbed onto Hg [59,60]. The complexation of Ti^+ by Gramicidin can be considered as the chemical step before the reduction. This CE process is reasonably expected for Gramicidin since it is a selective ion channel. Without specific information on binding sites for cations in the AmB pore, we limited our analysis to a simple determination of the size and density of pores, keeping in mind that the possibility of aggregation of smaller pores into larger patches cannot be distinguished from a patch-sized pore.

Characterization of the porosity of the layers as a function of the transmembrane potential allowed for investigation of the effect of potential on the integrity of the adsorbed lipid layer, and the influence the drug had on these monolayers. Fig. 4 shows the current–potential relationship 50 ms after the potential step as a function of 80% TD of the drug formulations (Fig. 4a is the Abelcet group, Fig. 4b the FZ group). All currents are normalized to the linear diffusion limited value. In both Fig. 4a and b, the pure DOPC layer blocks the Ti^+ transport until 100 mV positive of the potential-induced phase transition, where the current quickly increases to match the diffusion-limited value. No transport of Ti^+ through the DOPC layer was measured for potentials even 300 mV negative of the reversible potential ($\sim -450\ \text{mV}$) illustrating the highly organized defect-free nature of the DOPC monolayer on Hg. This has been reported previously [42]. The increase in the current flowing through the DOPC layer modified by interaction with the drug in the subphase directly indicates the porosity of the lipid monolayer. As seen in Fig. 4a, the Abelcet blank slightly positively shifts the break through potential. Abelcet also positively shifts the break through potential. No significant changes were observed for the Abelcet group in the potential region before the onset of the phase transition. This

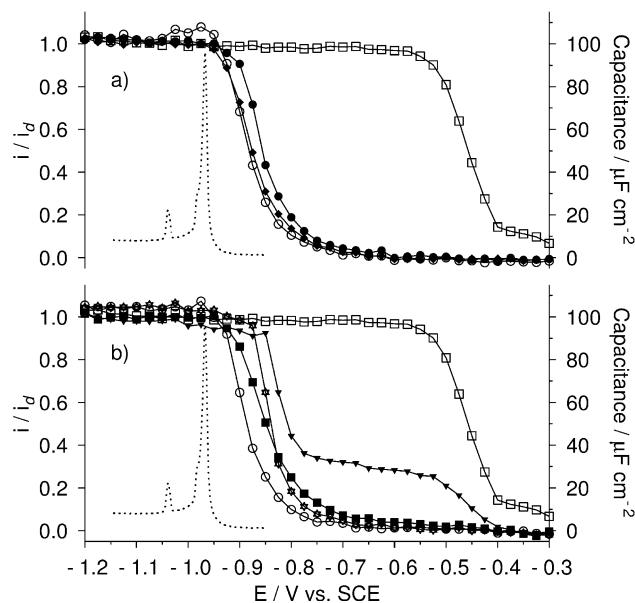


Fig. 4. Normalized Ti^+ reduction currents for a DOPC-coated Hg drop in contact with various formulations of AmB (80% of TD or equivalent). The capacitance of the DOPC monolayer is shown for reference (---). □ No DOPC, ○ DOPC, ■ deoxycholate, ☆ FZ, ▼ HFZ, ◆ Abelcet blank, ● Abelcet.

supports the minimum capacity measurements that indicate an undisturbed DOPC monolayer at these potentials. Fig. 4b illustrates the significant changes brought about by interaction of DOPC with the FZ group. The deoxycholate blank has an impact on the porosity of the DOPC monolayer in a similar fashion as observed for Abelcet. A more significant shift in the break through potential was observed for FZ indicating that the monolayer was defected or poorly organized due to interaction with FZ. Interaction with the HFZ resulted in a very porous layer with significant current measured at potentials just negative of the reversible Ti reduction potential. This has been observed previously for Ti^+ transport through incorporated Gramicidin [42].

Quantification of these observations was accomplished by fitting the random hole model to the current transients resulting in values for the mean radius of the pore (r_{active}), the average density of pores (N) and the fraction of surface covered by lipid (θ). These parameters are plotted in Fig. 5 as a function of the TD for a potential near the complete opening of the layer, $-850\ \text{mV/SCE}$. The error bars represent the average standard deviation for each set of data except HFZ (which is explained later). At this potential, the greatest changes due to interaction with the drug are observed. The data are separated into the Abelcet and FZ groups, and characterize the as-formed layers. The Abelcet group consists of the lipid blank and Abelcet. Abelcet displays slightly larger holes and density of holes than does the blank. In both cases, the size of the holes increase with %TD, and the density slightly decreases. The calculated coverage of lipid is close to 1 for the blank, but a consistently smaller coverage was measured for Abelcet. In

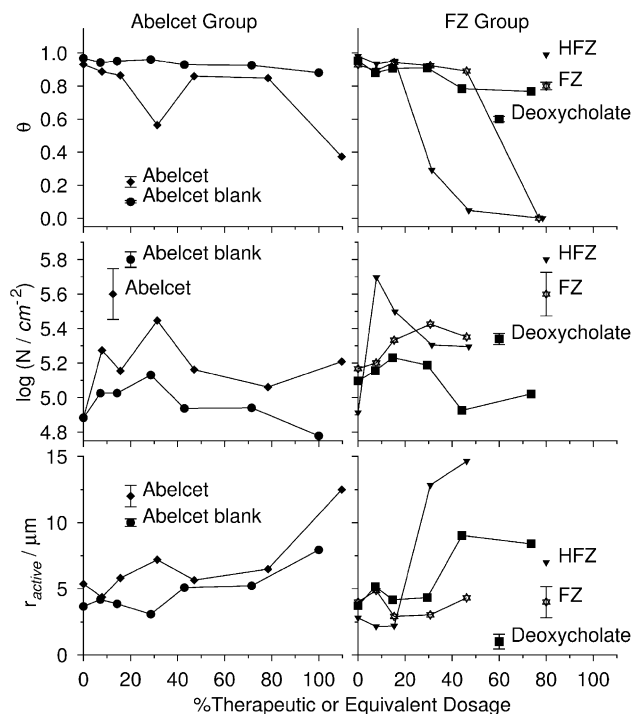


Fig. 5. Calculated pore size (bottom), density (middle) and lipid coverage (top) for the various formulations of AmB as a function of the fraction of TD or equivalent: ■ deoxycholate, ☆ FZ, ▼ HFZ, ◆ Abelcet blank, ● Abelcet.

fact, a decrease in lipid coverage was observed for Abelcet at the 30% TD value. A similar change was observed for the capacitive peak maximum measurements presented in Fig. 3 where the strongest decrease in peak height was observed around this value. This suggests that Abelcet/DOPC may interact strongly at this ratio introducing holes or defects in the monolayer. The measured pores are 5–15 μm in size which is similar to the structures observed in lipid monolayers at the gas/solution interface [61,62] suggesting that the pores measured using our technique may represent porous patches within our lipid monolayer. Recent AFM measurements of AmB interaction with lipid bilayer on mica also report regions <1 μm in diameter that are believed to be AmB pores [11]. Many of these structures exist close together possibly creating an even larger patch similar to our measurements.

The FZ group contains the fitting results for deoxycholate, FZ and HFZ. The data presented in Fig. 5b do not cover the full TD range. The FZ and HFZ at high TD (> 50%) are very porous and linear diffusion profiles result preventing an estimate of the coverage or hole size and density. For coverage values below ~ 0.5 , large deviations in the fitting parameters were observed and therefore the average standard deviation for HFZ is not shown. Deoxycholate was only characterized to 80%TD. Deoxycholate interacted with the DOPC monolayer yielding hole radii and densities similar to that observed for Abelcet. An increase in hole size was observed for TD values greater than 40%, also

reflected in the coverage. FZ gave values very similar to deoxycholate, though the layer was less porous at 40% TD. Above this value of TD, the lipid layer was strongly porated. The largest disturbance in the integrity of the monolayer was observed for HFZ. The average hole size sharply increased for values above 20% TD. The hole density was larger than deoxycholate and FZ, but only slightly. The coverage strongly declined starting at 20% TD. These data illustrate the disruptive effect of HFZ on a pure DOPC monolayer, disrupting and porating the DOPC monolayer at moderate fractions of the TD or equivalent. FZ is heat treated to reduce toxicity, but our HFZ results demonstrate a larger disruptive influence on pure DOPC monolayer as compared to FZ. In contrast to the toxicity studies on HFZ, our measurements were performed on sterol-free lipid monolayers. The future addition of sterol into the lipid monolayer will allow us to probe the sterol/AmB hypothesis. These experiments are in progress.

The TI data correlate well with the capacitance observations described previously. In both blank tests, the lipid monolayer was essentially unchanged for Abelcet blank, and moderately disrupted in the presence of deoxycholate. Abelcet does interact with the DOPC monolayer at intermediate TD values, but generally, the DOPC monolayer remained intact. FZ and HFZ had the largest destructive effects on lipid monolayer, and for values >40% TD, the lipid layer was destroyed, offering no impediment to metal ion reduction. In all cases, the formulation containing AmB was significantly more disruptive to the DOPC monolayer than the corresponding blank experiments, illustrating that AmB is a major contributor to the disorganization and destruction of the lipid layer.

4. Conclusions

A model system was used to study the interaction of three formulations of AmB with a lipid monolayer. The character of the interaction was interrogated utilizing electrochemical techniques sensitive to the organizational state of the lipid monolayer. The model system was sensitive to changes in the lipid layer due to the interaction with various formulations of AmB. The largest disruptive interaction was observed for the FZ and HFZ formulations. Deoxycholate (FZ blank) weakly interacted with the lipid layer, significantly less than when present with AmB. The lipid AmB complex, Abelcet, demonstrated a much lower disruptive effect toward the lipid monolayer, although the amount of AmB in the subphase was 10 times larger when compared to FZ. The Abelcet blank did not significantly influence the character of the DOPC monolayer. The lipid present in the Abelcet may have a shielding, annealing and/or healing effect that buffers the disruption due to the presence of AmB. Utilizing this model system, we plan to investigate the interaction of these formulations of AmB with DOPC layers modified by the addition of cholesterol and ergo-

sterol. The activity of AmB toward the sterol-containing monolayer and as a function of formulation of the drug will be measured. Interrogation of AmB/sterol/lipid interactions by capacitance and measurement of pore sizes and density will be performed and compared to these sterol-free measurements.

Acknowledgements

This work was performed with financial support from NSERC, and the Canadian Institutes of Health Research Grant no. MOP-14484. R.S. acknowledges support from NSERC in the form of a UGSF and support from BC Summer Works.

References

- [1] D.A. Rothon, R.G. Mathias, M.T. Schechter, *Can. Med. Assoc. J.* 151 (1994) 781–787.
- [2] R.N. Jones, *Diagn. Microbiol. Infect. Dis.* 25 (1996) 153–161.
- [3] C.A. Lyman, T.J. Walsh, *Drugs* 44 (1992) 9–35.
- [4] E.S. Dodds, R.H. Drew, J.R. Perfect, *Pharmacotherapy* 20 (2000) 1335–1355.
- [5] G.P. Bodey, *Am. J. Med.* 81 (1986) 11–26.
- [6] V. Joly, J. Bolard, P. Yeni, *Antimicrob. Agents Chemother.* 36 (1992) 1799–1804.
- [7] A.M. Gardier, D. Mathe, X. Guedeney, *Ther. Drug Monit.* 15 (1993) 274–280.
- [8] S. Schreier, S.V.P. Malheiros, E. de Paula, *Biochim. Biophys. Acta* 1508 (2000) 210–234.
- [9] J. Bolard, V. Joly, P. Yeni, *J. Liposome Res.* 3 (1993) 409–427.
- [10] R.A. Brutyan, P. McPhie, *J. Gen. Physiol.* 107 (1996) 69–78.
- [11] J. Milhaud, V. Ponsinet, M. Takashi, B. Michels, *Biochim. Biophys. Acta* 1558 (2002) 95–108.
- [12] D. Romanini, G. Avalue, B. Nerli, G. Pico, *Biophys. Chem.* 77 (1999) 69–77.
- [13] F. Gaboriau, M. Cheron, C. Petit, J. Bolard, *Antimicrob. Agents Chemother.* 41 (1997) 2345–2351.
- [14] E.H. Kwong, M. Ramaswamy, E.A. Bauer, S.C. Hartsel, K.M. Wasan, *Antimicrob. Agents Chemother.* 45 (2001) 2060–2063.
- [15] C. Gates, R.J. Pinney, *J. Clin. Pharm. Ther.* 18 (1993) 147–153.
- [16] R.J. Hay, *J. Infect.* 28 (1994) 35–43.
- [17] F. Meunier, *J. Infect.* 28 (1994) 51–56.
- [18] R.A. Frumtling, *Drugs Future* 20 (1995) 129–141.
- [19] S. de Marie, *Leukemia* 10 (Suppl. 2) (1996) s93–s96.
- [20] Y. Aracava, S. Schreier, R. Phadke, R. Deslauriers, I.C.P. Smith, *Biophys. Chem.* 14 (1981) 325–332.
- [21] J. Milhaud, M.A. Hartmann, J. Bolard, *Biochimie* 71 (1989) 49–56.
- [22] T. Ruckwardt, A. Scott, J. Scott, P. Mikulecky, S.C. Hartsel, *Biochim. Biophys. Acta* 1372 (1998) 283–288.
- [23] J. Minones, O. Conde, R. Seoane, P. Dynarowicz-Latka, *Langmuir* 16 (2000) 5743–5748.
- [24] I. Rey-Gomez-Serranillos, P. Dynarowicz-Latka, J. Minones, R. Seoane, *J. Colloid Interface Sci.* 234 (2001) 351–355.
- [25] J. Minones Jr., J. Minones, O. Conde, R. Seoane, P. Dynarowicz-Latka, *Prog. Colloid & Polym. Sci.* 112 (1999) 23–28.
- [26] Y. Saka, T. Mita, *J. Biochem.* 123 (1998) 798–805.
- [27] J. Barwicz, P. Tancrede, *Chem. Phys. Lipids* 85 (1997) 145–155.
- [28] K. Wojtowicz, W.I. Gruszecki, M. Walicka, J. Barwicz, *Biochim. Biophys. Acta* 1373 (1998) 220–226.
- [29] R. Seoane, J. Minones, O. Conde, M. Casas, E. Iribarnegaray, *Biochim. Biophys. Acta* 1375 (1998) 73–83.
- [30] M. Saint-Pierre-Chazalet, C. Thomas, M. Dupeyrat, C.M. Gary-Bobo, *Biochim. Biophys. Acta* 944 (1988) 477–486.
- [31] J. Minones, C. Carrera, P. Dynarowicz-Latka, O. Conde, R. Seoane, J.M.R. Patino, *Langmuir* 17 (2001) 1477–1482.
- [32] M.P.N. Gent, J.H. Prestegard, *Biochim. Biophys. Acta* 426 (1976) 17–30.
- [33] B.D. Wolf, S.C. Hartsel, *Biochim. Biophys. Acta* 1238 (1995) 156–162.
- [34] C. Salerno, E. Capuozzo, C. Crifo, *J. Liposome Res.* 3 (1993) 671–678.
- [35] B. Eleazar Cohen, *Biochim. Biophys. Acta* 857 (1986) 117–122.
- [36] P.J. Aggett, P.K. Fenwick, H. Kirk, *Biochim. Biophys. Acta* 684 (1982) 291–294.
- [37] T. Teerlink, B. De Kruijff, R.A. Demel, *Biochim. Biophys. Acta* 599 (1980) 484–492.
- [38] H. Ramos, E. Valdivieso, M. Gamargo, F. Dagger, B.E. Cohen, *J. Membr. Biol.* 152 (1996) 65–75.
- [39] H. Ramos, A. Attias de Murciano, B.E. Cohen, J. Bolard, *Biochim. Biophys. Acta* 982 (1989) 303–306.
- [40] A. Nelson, F.A.M. Leermakers, *J. Electroanal. Chem.* 278 (1990) 73–83.
- [41] F.A.M. Leermakers, A. Nelson, *J. Electroanal. Chem.* 278 (1990) 53–72.
- [42] D. Bizzotto, A. Nelson, *Langmuir* 14 (1998) 6269–6273.
- [43] M.R. Moncelli, L. Becucci, A. Nelson, R. Guidelli, *Biophys. J.* 70 (1996) 2716–2726.
- [44] A. Nelson, *Langmuir* 12 (1996) 2058–2067.
- [45] A. Nelson, N. Auffret, J. Borlakoglu, *Biochim. Biophys. Acta* 1021 (1990) 205–216.
- [46] W. Lorenz, F. Möckel, *Z. Elektrochem.* 60 (1956) 507–515.
- [47] W. Lorenz, *Z. Phys. Chem.* 18 (1958) 1–10.
- [48] W. Lorenz, W. Müller, *Z. Phys. Chem.* 18 (1958) 141–146.
- [49] A. Nelson, N. Auffret, *J. Electroanal. Chem.* 248 (1988) 167.
- [50] I.R. Miller, in: G. Milazzo (Ed.), *Topics in Biochemistry and Bioenergetics*, vol. 4, Wiley, New York, 1981, pp. 161–224.
- [51] G.L. Gaines Jr., *Insoluble Monolayers*, Interscience, New York, 1966.
- [52] Z. Galus (Ed.), *Fundamentals of Electrochemical Analysis*, Ellis Horwood, Chichester, 1976.
- [53] K.M. Abusalah, *Br. J. Biomed. Sci.* 53 (1996) 122–133.
- [54] B.R. Scharifker, *J. Electroanal. Chem.* 240 (1988) 61–76.
- [55] G. Pyzik, J. Lipkowski, *J. Electroanal. Chem.* 123 (1981) 351.
- [56] M. Golezdzinowski, J. Dojlido, J. Lipkowski, *J. Phys. Chem.* 89 (1985) 3506.
- [57] J. Lipkowski, C. Buess-Herman, J. Lambert, L. Gierst, *J. Electroanal. Chem.* 202 (1986) 169.
- [58] J. Lipkowski, in: B.E. Conway, J.O'M. Bockris, R.E. White (Eds.), *Modern Aspects of Electrochemistry*, vol. 23, Plenum, New York, 1992, pp. 1–99.
- [59] A. Nelson, D. Bizzotto, *Langmuir* 15 (1999) 7031–7039.
- [60] A. Nelson, *Biophys. J.* 80 (2001) 2694–2703.
- [61] C.W. McConlogue, T.K. Vanderlick, *Langmuir* 13 (1997) 7158–7164.
- [62] D. Mobius, *Curr. Opin. Colloid Interface Sci.* 1 (1996) 250–256.